

2 **Boundary Layer Effect in BEM with High Order** 3 **Geometry Elements Using Transformation**

4 **Y.M. Zhang¹, Y. Gu¹ and J.T. Chen²**

5 **Abstract:** The accurate evaluation of nearly singular integrals is one of the major
6 concerned problems in the boundary element method (BEM). Although the current
7 methods have achieved great progress, it is often possible only for problems de-
8 fined in the simplest geometrical domains when the nearly singular integrals need
9 to be calculated. However, engineering processes occur mostly in complex geo-
10 metrical domains, and always, involve nonlinearities of the unknown variables and
11 its derivatives. Therefore, effective methods of dealing with nearly singular inte-
12 grals for such practical problems are necessary and need to be further investigated.
13 In this paper, a general strategy based on a nonlinear transformation is introduced
14 and applied to evaluate the nearly singular integrals in two dimensional (2D) elas-
15 ticity problems. The proposed nonlinear transformation method can figure out the
16 rapid variations of nearly singular kernels and extremely high accuracy of numer-
17 ical results can be achieved without increasing other computational efforts. The
18 accuracy and efficiency of the method are demonstrated through three examples
19 that are commonly encountered in the applications of the BEM.

20 **Keywords:** BEM, nearly singular integrals, transformation, high-order elements,
21 elasticity problem.

22 **1 Introduction**

23 Accurate and efficient evaluation of singular and nearly singular integrals is an
24 important issue in boundary element analysis. These integrands are singular func-
25 tions when the collocation point belongs to the integration elements, and many
26 effective methods [Atluri (2004), (2005); Atluri, Liu and Han (2006); Brebbia *et*
27 *al.* (1984); Chen (2002, 2000); Davies *et al.* (2007); Li, Wu and Yu (2009); Sanz
28 *et al.* (2007); Sun (1999); Tanaka, Sladek (1994); Guiggiani (1992); Gray *et al.*

¹ Institute of Applied Mathematics, Shandong University of Technology, Zibo 255049, P.R. China

² Department of Harbor and River Engineering, National Taiwan Ocean University, Keelung 20224, Taiwan

29 (2006); Young *et al.* (2007); Zhang and Wen (2004)] have been developed to deal
30 with them. If the collocation point is close to but not on the integration elements,
31 the ensuring integrals are termed nearly weak singular, nearly strong singular and
32 nearly hyper-singular integrals, which are not singular in the sense of mathemat-
33 ics. However, from the point of view of numerical integrations, these integrals can
34 not be calculated accurately by using the standard Gaussian quadrature. This is
35 so-called boundary layer effect in BEM.

36 The accurate evaluation of nearly singular integrals plays an important role in many
37 engineering problems. In general, these include evaluating the solution near the
38 boundary in potential problems and calculating displacements and stresses near
39 the boundary in elasticity problems, for example, contact problems, displacement
40 around crack tips, sensitivity problems and thin-body problems [Chen and Liu
41 (2001); Albuquerque and Aliabadi (2008); Guz *et al.* (2007); Karlis *et al.* (2008)].

42 Owing to the importance of the nearly singular integrals, a great amount of at-
43 tention has been attracted and many numerical methods and techniques have been
44 developed in recent years. The proposed methods include, but are not limited to,
45 virtual boundary element method [Sun (1999); Zhang and Sun (2000)], rigid-body
46 displacement method or the simple solution method [Chen *et al.* (1998); Cruse
47 (1974); Lachat and Watson (1976); liu *et al.* (2008); Wang *et al.* (1994); Mukerjee
48 (2000); Sladek and Tanaka (1993); Granados and Gallego (2001)], interval subdi-
49 vision method [Jun (1985); Tanaka (1991); Gao (2008)], special Gaussian quadra-
50 ture method [Earlin (1992); Lifeng (2004)], analytical or semi-analytical methods
51 [Yoon and Heister (2000); Zhang and Sun (2001); Friedrich (2002); Fratantonio
52 and Rencis (2000); Zhang and Zhang (2004); Cruse and Aithal (1993); Schulz
53 (1998); Liu (1998); Zhou *et al.* (2008); Niu (2007)]. In a recent study, the above
54 methods have been reviewed in detail by Zhang *et al.* [Zhang and Sun (2008)].

55 At present, the most common methods for calculating nearly singular integrals are
56 various nonlinear transformations, for example, the cubic polynomial transforma-
57 tion [Telles (1987)], the bi-cubic transformation [Cerroloza and Alarcon (1989)],
58 the sigmoidal transformation [Johnston (1999)], the semi-sigmoidal transforma-
59 tion [Johnston (2000)], the coordinate optimization transformation [Sladek, Sladek
60 and Tanaka (2000)], the attenuation mapping method [Earlin (1993); Luo *et al.*
61 (1998)], the rational transformation [Huang and Cruse (1993)], and the distance
62 transformation [Ma and Kamiya (2002)]. The basic ideas of the above transforma-
63 tions can be generalized into two categories: one is removing the nearly zero factor
64 by using another zero factor which usually generated by Jacobian; the other one is
65 converting the nearly zero factor in the denominator to be part of the numerator,
66 which profits from the idea of the reciprocal transformation for the regularization
67 of weakly singular integrals. Numerical tests show that the transformations based

68 on the former idea are effective for the calculation of weakly singular integrals but
69 not satisfactory for strong singular or hypersingular integrals. The latter transfor-
70 mations, based on the idea of reciprocal transformation, can convert nearly singular
71 kernels into regular kernels, but the original regular parts behave nearly singular af-
72 ter the transformations, so they are suitable only for a case when the regular part of
73 the integrand is constant.

74 For most of current numerical methods, the geometry of the boundary element is
75 often depicted by using linear shape functions when nearly singular integrals need
76 to be calculated. However, most engineering processes occur mostly in complex
77 geometrical domains, and obviously, higher order geometry elements are expected
78 to be more accurate [Atluri (2005)]. To improve the calculation accuracy and ef-
79 ficiency of the nearly singular integrals, efficient approaches for estimating nearly
80 singular integrals over high order geometry elements are necessary and need to be
81 further investigated.

82 When the geometry of the boundary element is approximated by using high order
83 elements—usually of second order, the Jacobian $J(\xi)$ is not a constant but a non-
84 rational function which can be expressed as $\sqrt{a + b\xi + c\xi^2}$, where a, b and c are
85 constants, ξ is the dimensionless coordinate; The distance r between the field points
86 and the source point is a non-rational function of the type $\sqrt{p_4(\xi)}$, where $p_4(\xi)$
87 is the fourth order polynomial. Thus, the forms of the integrands in boundary
88 integrals become more complex, and it is, generally, more difficult to implement
89 when nearly singular integrals need to be calculated.

90 This paper aims to develop a general strategy suitable for calculating the nearly
91 singular integrals occurring on high order geometry elements. A general nonlinear
92 transformation technique [Zhang and Sun (2008)] is adopted to remove the near
93 singularities of kernels' integration by smoothing out the rapid variations of the
94 integrand of nearly singular integrals. The strategy proposed in this paper adopted
95 isoparametric quadratic elements to describe the integral kernel functions and the
96 Jacobean. Owing to the employment of the parabolic arc, only a small number of
97 elements need to be divided along the boundary, and high accuracy can be achieved
98 without increasing more computational efforts. In addition, the non-singular BIEs
99 of indirect variables [Zhang and Wen (2004)] were employed to estimate the singu-
100 lar integrals occurring on curved boundaries. Three numerical examples of elastic
101 problems are given, with results, showing the high efficiency and the stability of
102 the suggested approach, even when the internal point is very close to the boundary.

103 **2 Non-singular boundary integral equations (BIEs)**

104 It is well known that the domain variables can be computed by integral equations
 105 only after all the boundary quantities have been obtained, and the accuracy of
 106 boundary quantities directly affects the validity of the interior quantities. How-
 107 ever, when calculating the boundary quantities, we have to deal with the singular
 108 boundary integrals, and a good choice is using the regularized BIEs. Therefore, for
 109 avoiding the “boundary layer effect”, two aspects are necessary. One is the accurate
 110 computation of the boundary functions, which is generally carried out by adopting
 111 the regularized BIEs; the other is an efficient algorithm of calculating the nearly
 112 singular integrals.

In this paper, we always assume that Ω is a bounded domain in R^2 , Ω^c is its open complement, and Γ denotes the boundary. $\mathbf{t}(\mathbf{x})$ and $\mathbf{n}(\mathbf{x})$ (or \mathbf{t} and \mathbf{n}) are the unit tangent and outward normal vectors of Γ to the domain Ω at the point \mathbf{x} , respectively. For 2D elastic problems, the non-singular BIEs with indirect variables are given in [Zhang and Wen (2004)]. Without regard to the rigid body displacement and the body forces, the non-singular BIEs on Ω^c can be expressed as

$$u_i(\mathbf{y}) = \int_{\Gamma} \varphi_k(\mathbf{x}) u_{ik}^*(\mathbf{y}, \mathbf{x}) d\Gamma, \mathbf{y} \in \Gamma \tag{1}$$

$$\begin{aligned} \nabla u_i(\mathbf{y}) = & \int_{\Gamma} [\varphi_k(\mathbf{x}) - \varphi_k(\mathbf{y})] \nabla u_{ik}^*(\mathbf{y}, \mathbf{x}) d\Gamma - \varphi_k(\mathbf{y}) \left\{ \int_{\Gamma} [\mathbf{t}(\mathbf{x}) - \mathbf{t}(\mathbf{y})] \frac{\partial u_{ik}^*(\mathbf{y}, \mathbf{x})}{\partial \mathbf{t}} d\Gamma \right. \\ & + \int_{\Gamma} [\mathbf{n}(\mathbf{x}) - \mathbf{n}(\mathbf{y})] \frac{\partial u_{ik}^*(\mathbf{y}, \mathbf{x})}{\partial \mathbf{n}} d\Gamma + \frac{k_0}{G} \mathbf{n}(\mathbf{y}) \left(\int_{\Gamma} [n_k(\mathbf{x}) - n_k(\mathbf{y})] \frac{\partial \ln r}{\partial x_i} d\Gamma \right. \\ & \left. \left. + n_k(\mathbf{y}) \int_{\Gamma} [t_i(\mathbf{x}) - t_i(\mathbf{y})] \frac{\partial \ln r}{\partial \mathbf{t}} d\Gamma + n_k(\mathbf{y}) \int_{\Gamma} [n_i(\mathbf{x}) - n_i(\mathbf{y})] \frac{\partial \ln r}{\partial \mathbf{n}} d\Gamma \right) \right\}, \\ & \mathbf{y} \in \Gamma \end{aligned} \tag{2}$$

For the domain Ω , the nonsingular BIEs are given as

$$u_i(\mathbf{y}) = \int_{\Gamma} \varphi_k(\mathbf{x}) u_{ik}^*(\mathbf{x}, \mathbf{y}) d\Gamma, \mathbf{y} \in \Gamma \tag{3}$$

$$\begin{aligned}
 \nabla u_i(\mathbf{y}) = & \phi_k(\mathbf{y})\mathbf{n}(\mathbf{y}) \frac{1}{G} \left[\delta_{ik} - \frac{n_k(\mathbf{y})n_i(\mathbf{y})}{2(1-\nu)} \right] + \int_{\Gamma} [\phi_k(\mathbf{x}) - \phi_k(\mathbf{y})] \nabla u_{ik}^*(\mathbf{y}, \mathbf{x}) d\Gamma \\
 & - \phi_k(\mathbf{y}) \left\{ \int_{\Gamma} [\mathbf{t}(\mathbf{x}) - \mathbf{t}(\mathbf{y})] \frac{\partial u_{ik}^*(\mathbf{y}, \mathbf{x})}{\partial \mathbf{t}} d\Gamma + \int_{\Gamma} [\mathbf{n}(\mathbf{x}) - \mathbf{n}(\mathbf{y})] \frac{\partial u_{ik}^*(\mathbf{y}, \mathbf{x})}{\partial \mathbf{n}} d\Gamma \right. \\
 & + \frac{k_0}{G} \mathbf{n}(\mathbf{y}) \left(\int_{\Gamma} [n_k(\mathbf{x}) - n_k(\mathbf{y})] \frac{\partial \ln r}{\partial x_i} d\Gamma + n_k(\mathbf{y}) \int_{\Gamma} [t_i(\mathbf{x}) - t_i(\mathbf{y})] \frac{\partial \ln r}{\partial \mathbf{t}} d\Gamma \right. \\
 & \left. \left. + n_k(\mathbf{y}) \int_{\Gamma} [n_i(\mathbf{x}) - n_i(\mathbf{y})] \frac{\partial \ln r}{\partial \mathbf{n}} d\Gamma \right) \right\}, \\
 & \mathbf{y} \in \Gamma
 \end{aligned} \tag{4}$$

For the internal point \mathbf{y} , the integral equations can be written as

$$u_i(\mathbf{y}) = \int_{\Gamma} \phi_k(\mathbf{x}) u_{ik}^*(\mathbf{y}, \mathbf{x}) d\Gamma, \quad \mathbf{y} \in \hat{\Omega} \tag{5}$$

$$\nabla u_i(\mathbf{y}) = \int_{\Gamma} \phi_k(\mathbf{x}) \nabla u_{ik}^*(\mathbf{y}, \mathbf{x}) d\Gamma, \quad \mathbf{y} \in \hat{\Omega} \tag{6}$$

113 In Eqs. (1)–(6), $i, k = 1, 2$; $k_0 = 1/4\pi(1 - \nu)$; G is the shear modulus; $\phi_k(\mathbf{x})$ is
 114 the density function to be determined; $u_{ik}^*(\mathbf{y}, \mathbf{x})$ denotes the Kelvin fundamental
 115 solution. In Eqs. (5) and (6) $\hat{\Omega} = \Omega$ or Ω^c .

When the field point \mathbf{y} is far from the boundary element, a straightforward application of Gaussian quadrature suffices to evaluate such integrals. However, when the field point \mathbf{y} is very close to the integral element Γ_e , the distance r between the field point \mathbf{y} and the source point \mathbf{x} tends to zero. Thus, there exist nearly singular integrals in Eqs. (5) and (6). These nearly singular integrals can be expressed as

$$\begin{cases} I_1 = \int_{\Gamma_e} \psi(\mathbf{x}) \ln r^2 d\Gamma \\ I_2 = \int_{\Gamma_e} \psi(\mathbf{x}) \frac{1}{r^{2\alpha}} d\Gamma \end{cases} \tag{7}$$

116 where $\alpha > 0$, $\psi(\mathbf{x})$ denotes a well-behaved function.

117 3 Nearly singular integrals under curvilinear elements

118 The quintessence of the BEM is to discretize the boundary into a finite number
 119 of segments, not necessarily equal, which are called boundary elements. Two approximations are made over each of these elements. One is about the geometry of
 120 the boundary, while the other has to do with the variation of the unknown boundary quantity over the element. The linear element is not an ideal one as it can not
 121 approximate with sufficient accuracy for the geometry of curvilinear boundaries.
 122
 123

124 For this reason, it is recommended to use higher order elements, namely, elements
 125 that approximate geometry and boundary quantities by higher order interpolation
 126 polynomials—usually of second order. In this paper, the geometry segment is mod-
 127 eled by a continuous parabolic element, which has three knots, two of which are
 128 placed at the extreme ends and the third somewhere in-between, usually at the mid-
 129 point. Therefore the boundary geometry is approximated by a continuous piece-
 130 wise parabolic curve. On the other hand, the distribution of the boundary quantity
 131 on each of these elements is depicted by a discontinuous quadratic element, three
 132 nodes of which are located away from the endpoints.

Assume $\mathbf{x}^1 = (x_1^1, x_2^1)$ and $\mathbf{x}^2 = (x_1^2, x_2^2)$ are the two extreme points of the segment Γ_j , and $\mathbf{x}^3 = (x_1^3, x_2^3)$ is in-between one. Then the element Γ_j can be expressed as follows

$$x_k(\xi) = N_1(\xi)x_k^1 + N_2(\xi)x_k^2 + N_3(\xi)x_k^3, k = 1, 2$$

where $N_1(\xi) = \xi(\xi - 1)/2$, $N_2(\xi) = \xi(\xi + 1)/2$, $N_3(\xi) = (1 - \xi)(1 + \xi)$, $-1 \leq \xi \leq 1$. As shown in Fig. 1, the minimum distance d from the field point $\mathbf{y} = (y_1, y_2)$

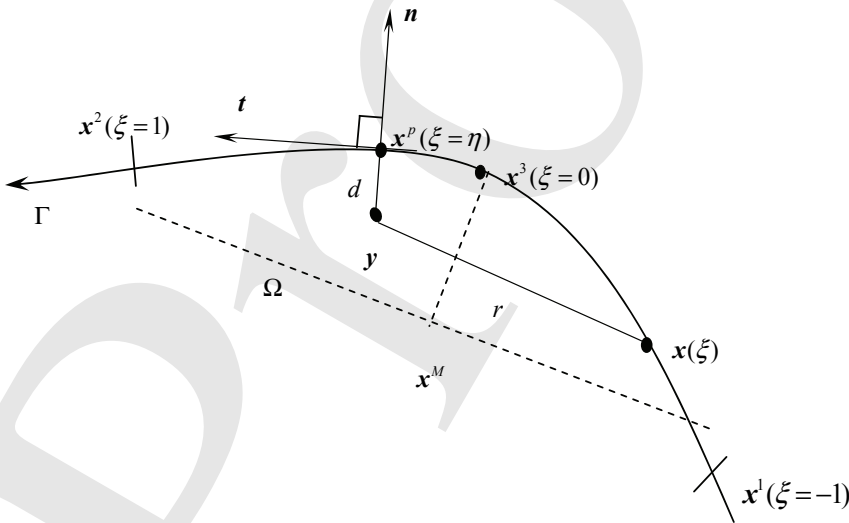


Figure 1: The minimum distance d from the field point \mathbf{y} to the boundary element

to the boundary element Γ_j is defined as the length of $\overline{\mathbf{y}\mathbf{x}^p}$, which is perpendicular to the tangential line \mathbf{t} and through the projection point \mathbf{x}^p . Letting $\eta \in (-1, 1)$ is the local coordinate of the projection point \mathbf{x}^p , i.e. $\mathbf{x}^p = (x_1(\eta), x_2(\eta))$. Then η is

the real root of the following equation

$$x'_k(\eta)(x_k(\eta) - y_k) = 0 \quad (8)$$

If the field point \mathbf{y} sufficiently approaches the boundary, then Eq. (8) has a unique real root. In fact, setting

$$F(\eta) = x'_k(\eta)(x_k(\eta) - y_k)$$

there is

$$F'(\eta) = x'_k(\eta)x'_k(\eta) + x''_k(\eta)(x_k(\eta) - y_k) = J^2(\eta) + x''_k(\eta)(x_k(\eta) - y_k)$$

133 where $J(\eta)$ is the Jacobian of the transformation from parabolic element to the
134 line interval $[-1, 1]$. Therefore, when the field point \mathbf{y} is sufficiently close to the
135 element, we explicitly have $F'(\eta) > 0$.

The unique real root of Eq. (8) can be evaluated numerically by using the Newton's method or computed exactly by adopting the algebraic root formulas of 3-th algebraic equations. In this paper, two ways are all tested, and practical applications show that both ways can be used to obtain desired results. Furthermore, the Newton's method is more simple and effective, especially if the initial approximation is properly chosen and if we can do this, only two or three iterations are sufficient to approximate the real root. For the root formula of 3-th algebraic equations, let's consider the following algebraic equation

$$ax^3 + bx^2 + cx + d = 0$$

if there exists only one real root, the analytical solution can be expressed as follows

$$x = -\frac{b}{3a} + \frac{2(\sqrt{s^2 + t^2})^{\frac{1}{3}}}{3\sqrt[3]{2a}} \cos\left(\frac{1}{3} \arccos \frac{s}{\sqrt{s^2 + t^2}}\right)$$

136 where $s = -2b^3 + 9acb - 27a^2d$, $t = \sqrt{-4(3ac - b^2)^3 - (-2b^3 + 9acb - 27a^2d)^2}$.

Using the procedures described above, we can obtain the value of the real root η . Thus, we have

$$\begin{aligned} x_k - y_k &= x_k - x_k^p + x_k^p - y_k \\ &= \frac{1}{2}(\xi - \eta) [(x_k^1 - 2x_k^3 + x_k^2)(\xi + \eta) + (x_k^2 - x_k^1)] + x_k(\eta) - y_k \end{aligned} \quad (9)$$

By using Eq. (9), the distance square r^2 between the field point \mathbf{y} and the source point $\mathbf{x}(\xi)$ can be written as

$$r^2(\xi) = (x_k - y_k)(x_k - y_k) = (\xi - \eta)^2 g(\xi) + d^2 \quad (10)$$

where $d^2 = (x_k(\eta) - y_k)(x_k(\eta) - y_k)$,

$$g(\xi) = \frac{1}{4}(x_k^1 - 2x_k^3 + x_k^2)(x_k^1 - 2x_k^3 + x_k^2)(\xi + \eta)^2 + \frac{1}{2}(x_k^1 - 2x_k^3 + x_k^2)(x_k^2 - x_k^1)(\xi + \eta) + h^2 + (x_k^1 - 2x_k^3 + x_k^2)(x_k(\eta) - y_k),$$

137 where $h = \frac{1}{2}\sqrt{(x_k^2 - x_k^1)(x_k^2 - x_k^1)}$.

138 Apparently, there is $g(\xi) \geq 0$.

By some simple deductions, the nearly singular integrals in Eq. (7) would be reduced to the following two types

$$I = \int_0^A f(\xi) \ln(\xi^2 g(\xi) + d^2) d\xi \tag{11}$$

$$II = \int_0^A \frac{f(\xi)}{(\xi^2 g(\xi) + d^2)^\alpha} d\xi \tag{12}$$

139 where A is a constant which is possibly with different values in different element
 140 integrals; $f(\cdot)$ is a regular function that consists of shape function, Jacobian and
 141 ones which arise from taking the derivative of the integral kernels.

142 4 Variable transformation

143 The main reason why nearly singular integrals can not be calculated accurately
 144 by using the standard Gaussian quadrature, in common observation, is caused by
 145 some bad qualities of the nearly singular kernels such as the fiercer oscillation and
 146 the unboundedness of the integrands. However, in the authors' opinion, that is not
 147 true. Some regular integral kernels, such as $\frac{x^2}{x^2+c^2}$ or $\frac{x^4}{x^2+c^2}$ which are obviously
 148 neither unbounded nor oscillating rapidly during the integral interval, still can not
 149 be calculated accurately by using the standard Gaussian quadrature (See Figs. 2
 150 and 3). For this phenomenon, we can also speculate that some methods such as
 151 attenuation mapping method, which eliminate the nearly zero factors by adopting
 152 another zero factors in the density function, would be not very effective, and the
 153 practices proved it. According to the authors' point of view, the main reason of
 154 this phenomenon is caused by the different orders of magnitude of the zero-divisor.
 155 In this section, a general variable transformation for high order boundary elements
 156 was constructed in order to diminish the difference of the orders of magnitude or
 157 the scale of change for operational factors. The constructed transformation can
 158 remove the near singularity efficiently and high accurate results can be obtained by
 159 using the standard Gaussian quadrature.

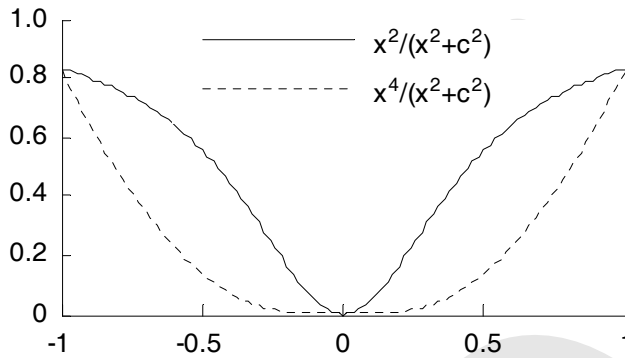


Figure 2: The images of two integral kernels with $c^2 = 0.2$

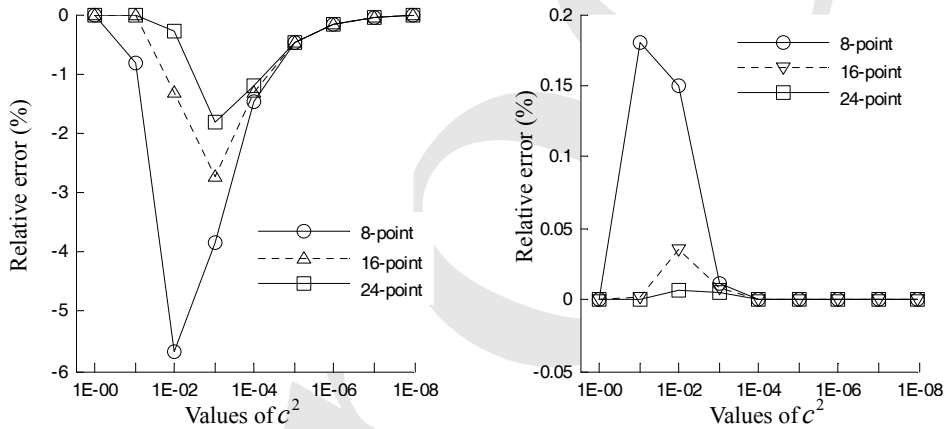


Figure 3: Relative errors of the computation results of $x^2/(x^2 + c^2)$ and $x^4/(x^2 + c^2)$ using 8-point/16-point/24-point Gaussian quadrature

Based on the idea of diminishing the difference of the orders of magnitude or the scale of changes of operational factors, we introduce the following transformation

$$\xi = d(e^{k(1+t)} - 1) \tag{13}$$

160 where $k = \frac{1}{2} \ln(1 + \frac{A}{d})$.

Substituting (13) into Eqs. (11) and (12), then we obtain the following equations

$$I = 2kd \ln d \int_{-1}^1 f(d(e^{k(1+t)} - 1)) e^{k(1+t)} dt + kd \int_{-1}^1 f(\xi) \ln \left((e^{k(1+t)} - 1)^2 g(\xi) + 1 \right) e^{k(1+t)} dt \quad (14)$$

$$\Pi = \frac{1}{d^{2\alpha-1}} \int_{-1}^1 \frac{f(\xi)}{\left((e^{k(1+t)} - 1)^2 g(\xi) + 1 \right)^\alpha} e^{k(1+t)} dt \quad (15)$$

161 where $\xi = d(e^{k(1+t)} - 1)$.

162 By following the procedures described above, the near singularity of the boundary
163 integrals has been fully regularized. The final integral formulations over parabolic
164 elements are obtained as shown in Eqs. (14) and (15), which can be computed
165 straightforward by using standard Gaussian quadrature.

166 5 Numerical examples

167 In this section, three examples of 2D elastostatics with curved boundaries are given
168 to test the proposed method. Isoparametric quadratic elements are employed to
169 approximate the geometrical elements and the boundary densities. The proposed
170 transformation technique is used to estimate the nearly singular integrals when the
171 interior points are very close to the integral elements.

172 **Example 1** As shown in Fig. 4, a thick cylinder subjected to the uniform radial
173 pressures $p = 5$ along the surfaces is considered. The inner and outer radii of the
174 cylinder are 1 and 2, respectively. In this example, the elastic shear modulus is
175 $G = 807692.3N/cm^2$, and the Poisson's ratio is $\nu = 0.3$.

176 Fifteen and ten quadratic elements are divided along the outer and inner surfaces,
177 respectively. Therefore, the total number of the elements is 25.

178 The numerical solutions of the tangential stresses σ_θ at the interior points close to
179 the outer and inner surfaces are listed in Tab. 1 and Tab. 2. Results of the radial
180 stresses σ_r at the interior points close to the outer and inner surfaces are listed
181 in Fig. 5 and Fig. 6, respectively. Both the CBEM and the proposed method are
182 employed for the purpose of comparison. The convergence rates of the computed
183 σ_θ at interior points $(1.0000001, 0)$ and $(1.9999999, 0)$ are shown in Fig.7.

184 It can be seen from Tab. 1 and Tab. 2 that the results of stresses σ_θ can be accurately
185 calculated by using the CBEM and the present method when the computed points
186 are not very close to the boundary ($r < 1.95$ or $r > 1.04$). However, when the
187 distance between the interior point and the boundary is equal to or less than 0.04,
188 the results calculated by the CBEM become less satisfactory or even invalid. In

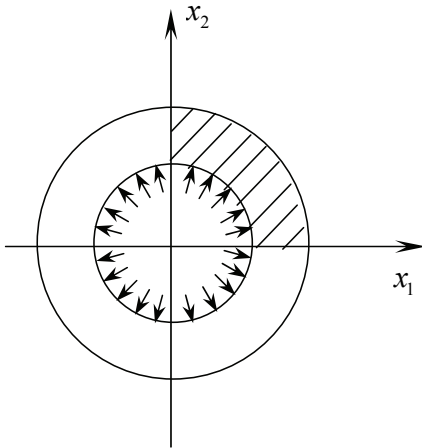


Figure 4: Thick cylinder subjected to the uniform radial pressure on the inner surface

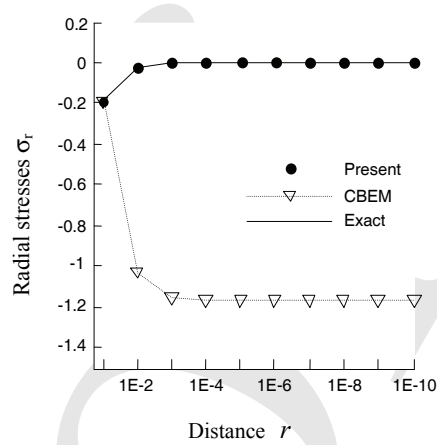


Figure 5: Radial stresses σ_r at interior points close to the outer surface

189 contrast with the CBEM, the present method can be used to obtain accurate results
 190 with the largest percentage error less than 0.1% even when the distance between
 191 the interior point and the outer boundary reaches 10^{-10} .

Table 1: Tangential stresses σ_θ at interior points

Radius r	Exact	CBEM	Present	Relative error
1.9	0.3513389E+01	0.3517443E+01	0.3513383E+01	0.1593349E-03
1.95	0.3419899E+01	0.3520995E+01	0.3418865E+01	0.3023558E-01
1.99	0.3350126E+01	0.3324564E+01	0.3347962E+01	0.6459433E-01
1.999	0.3335001E+01	0.2885692E+01	0.3332540E+01	0.7380650E-01
1.999 9	0.3333500E+01	0.2836292E+01	0.3331008E+01	0.7475973E-01
1.999 99	0.3333350E+01	0.2831348E+01	0.3330852E+01	0.7493745E-01
1.999 999	0.3333335E+01	0.2830854E+01	0.3330847E+01	0.7464263E-01
1.999 999 9	0.3333334E+01	0.2830804E+01	0.3330859E+01	0.7423208E-01
1.999 999 99	0.3333333E+01	0.2830799E+01	0.3330729E+01	0.7813735E-01
1.999 999 999	0.3333333E+01	0.2830799E+01	0.3330762E+01	0.7714073E-01
1.999 999 9999	0.3333333E+01	0.2830799E+01	0.3331151E+01	0.6546329E-01

192 We can observe from Fig. 5 and Fig. 6 that the results of radial stresses σ_r calcu-
 193 lated by using the CBEM become less satisfactory as the computed points locate
 194 increasingly close to the boundary, i.e., when the distance between the interior point

Table 2: Tangential stresses σ_θ at interior points close to the inner surface

Radius r	Exact	CBEM	Present	Relative error
1.1	0.7176309E+01	0.7177468E+01	0.7177468E+01	-0.1616178E-01
1.04	0.7830375E+01	0.7810632E+01	0.7833678E+01	-0.4218329E-01
1.01	0.8201974E+01	0.5963880E+01	0.8207646E+01	-0.6916232E-01
1.001	0.8320020E+01	0.1187044E+02	0.8326496E+01	-0.7783813E-01
1.0001	0.8332000E+01	0.1319104E+02	0.8338553E+01	-0.7864782E-01
1.00001	0.8333200E+01	0.1332452E+02	0.8339803E+01	-0.7923699E-01
1.000001	0.8333320E+01	0.1333787E+02	0.8339923E+01	-0.7923119E-01
1.0000001	0.8333332E+01	0.1333921E+02	0.8339887E+01	-0.7865526E-01
1.00000001	0.8333333E+01	0.1333934E+02	0.8338562E+01	-0.6274595E-01
1.000000001	0.8333333E+01	0.1333935E+02	0.8343783E+01	-0.1253925E+00
1.0000000001	0.8333333E+01	0.1333935E+02	0.8341133E+01	-0.9360174E-01

195 and the boundary is equal to or less than 0.05. By using the same mesh, the present
 196 method gains excellent accuracy even when the distance between the interior point
 197 and the outer boundary approaches 10^{-10} .

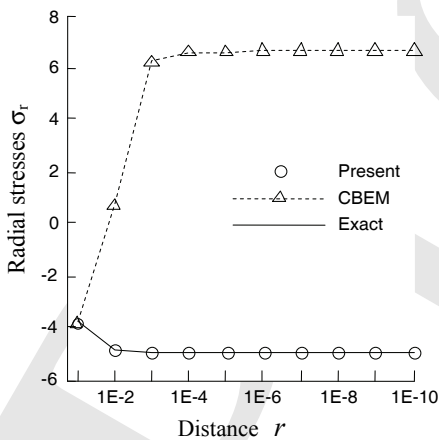


Figure 6: Radial stresses σ_r at interior points close to the inner surface

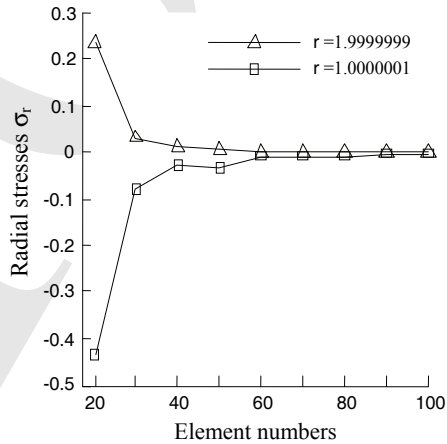


Figure 7: Convergence curves of the computed σ_θ

198 In addition, the convergence curves in Fig. 7 show that the convergence rates of the
 199 present method are fast even when the distance between the computed point and
 200 the boundary reaches 10^{-7} .

201 **Example 2** As shown in Fig. 8, an infinite plate with a circular hole subjected to

202 the uniform tensile forces $p = 2$ at infinity is considered. The radius of the circle
 203 is $r = 1$. In this example, the elastic shear modulus G and the Poisson's ratio ν are
 204 the same as in the example 1. There are 20 uniform quadratic boundary elements
 divided along the circular boundary.

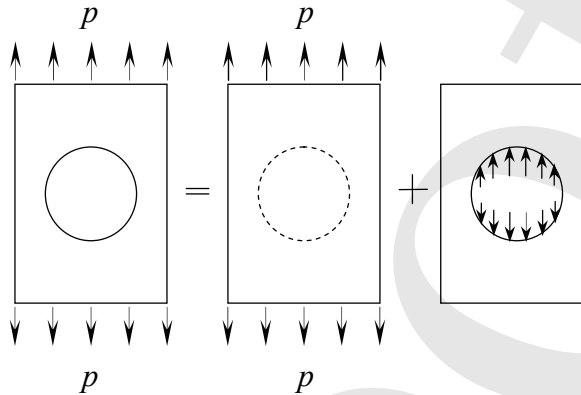


Figure 8: An infinite plate with a circular hole subjected to the uniform tensile forces

Table 3: Tangential stresses σ_θ at interior points on the line $x_2 = 0$

Coordinate x_1	Exact	CBEM	Present	Relative error
1.1	0.4875487E+01	0.4876466E+01	0.4876466E+01	-0.2009130E-01
1.01	0.5863237E+01	0.5805375E+01	0.5866426E+01	-0.5438222E-01
1.001	0.5986033E+01	0.6103824E+01	0.5989719E+01	-0.6157678E-01
1.0001	0.5998600E+01	0.6148594E+01	0.6002340E+01	-0.6234624E-01
1.00001	0.5999860E+01	0.6153027E+01	0.6003606E+01	-0.6243178E-01
1.000001	0.5999986E+01	0.6153470E+01	0.6003737E+01	-0.6251000E-01
1.0000001	0.5999999E+01	0.6153514E+01	0.6003735E+01	-0.6226901E-01
1.00000001	0.6000000E+01	0.6153518E+01	0.6003726E+01	-0.6210675E-01
1.000000001	0.6000000E+01	0.6153519E+01	0.6003862E+01	-0.6437451E-01
1.0000000001	0.6000000E+01	0.6153519E+01	0.6003715E+01	-0.6191998E-01

205

206 Tab. 3 presents the results of tangential stresses σ_θ calculated by using both the
 207 CBEM and the present method at interior points on the line $x_2 = 0$. It can be
 208 seen that the results calculated by the CBEM are not in a good agreement with the

Table 4: Tangential stresses σ_θ at interior points with the radius of $r = 1.000000001$

Angle θ	Exact	CBEM	Present	Relative error
0	0.6000000E+01	0.6153519E+01	0.6003862E+01	-0.6437451E-01
$\pi/10$	0.5236068E+01	0.5503660E+01	0.5239481E+01	-0.6518125E-01
$2\pi/10$	0.3236068E+01	0.3802308E+01	0.3238303E+01	-0.6906802E-01
$3\pi/10$	0.7639320E+00	0.1699320E+01	0.7647112E+00	-0.1019982E+00
$4\pi/10$	-0.1236068E+01	-0.2032196E-02	-0.1236467E+01	-0.3232167E-01
$5\pi/10$	-0.2000000E+01	-0.6518910E+00	-0.2000850E+01	-0.4251437E-01
$6\pi/10$	-0.1236068E+01	-0.2032196E-02	-0.1236469E+01	-0.3240459E-01
$7\pi/10$	0.7639320E+00	0.1699320E+01	0.7647094E+00	-0.1017558E+00
$8\pi/10$	0.3236068E+01	0.3802308E+01	0.3238301E+01	-0.6901786E-01
$9\pi/10$	0.5236068E+01	0.5503660E+01	0.5239480E+01	-0.6516227E-01
π	0.6000000E+01	0.6153519E+01	0.6003862E+01	-0.6437451E-01

209 analytic solutions as the computed points locate increasingly close to the boundary,
 210 i.e., when the distance between the interior point and the boundary is equal to or
 211 less than 0.01. However, the results calculated by the proposed method are very
 212 consistent with the exact solutions even when the distance between the interior
 213 point and the outer boundary approaches 10^{-10} . The percentage errors are also
 214 listed in Tab. 3, from which we can see that the accuracy of the results calculated
 215 by the present method are high and stable with the largest relative error less than
 216 0.07%.

217 For different angles, the calculation results of tangential stresses σ_θ at interior
 218 points with radius of 1.000000001 are listed in Tab. 4, from which we can observe
 219 that the results calculated by the CBEM become less satisfactory or even invalid. In
 220 contrast with the CBEM, the present method can be applied successfully to obtain
 221 accurate results at these interior points.

222 The results of radial stresses σ_r at interior points on the line $x_2 = 0$ are shown in Fig.
 223 9, from which we can see that the present method yields excellent accuracy even
 224 when the distance between the interior point and the inner surface reaches 10^{-10} .
 225 In addition, the convergence plot in Fig. 10 shows that the convergence rates of the
 226 present method are fast even when the distance between the computed point and
 227 the boundary approaches 10^{-9} .

228 **Example 3** An infinite plate with a circular hole subjected to a uniform radial
 229 pressure $p = 5$, as shown in Fig. 11. The radius of the circle is $r = 5$. In this
 230 example, the elastic shear modulus G and the Poisson's ratio ν are the same as in
 231 the example 1.

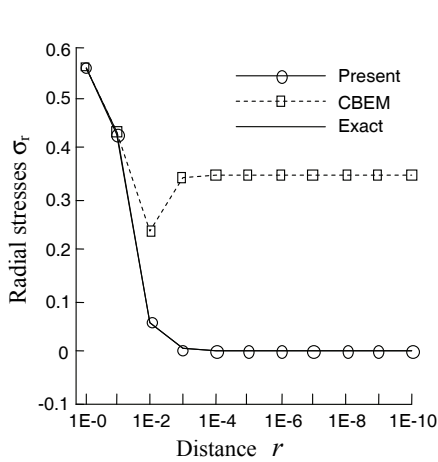


Figure 9: Radial stresses σ_r at interior points on the line $x_2 = 0$

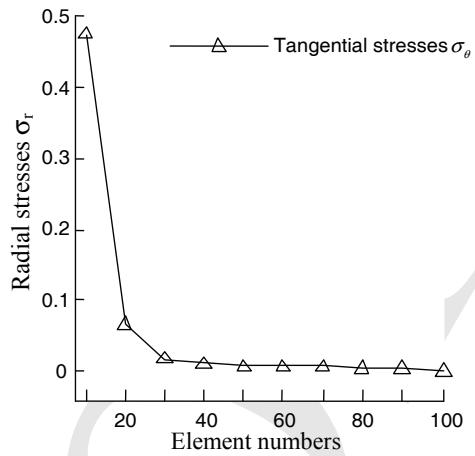


Figure 10: Convergence curve of the computed σ_θ at the point $(1E-09, 0)$

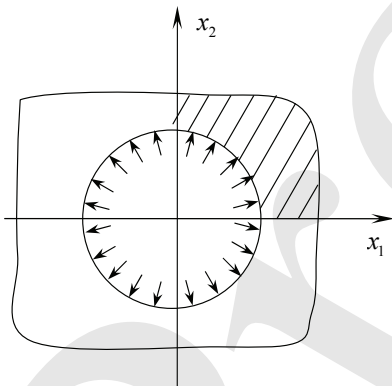


Figure 11: An infinite plate with a circular hole subjected to a uniform radial pressure

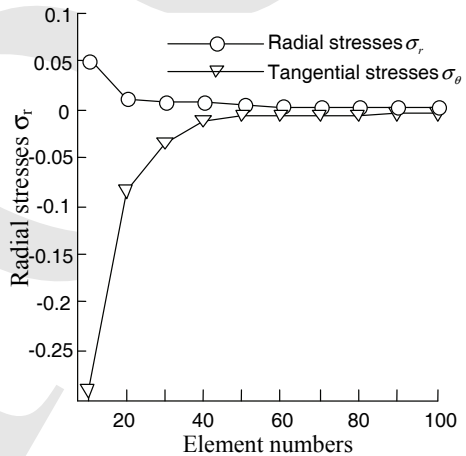


Figure 12: Convergence curves of the stresses σ_r and σ_θ at the point $(5E-07, 0)$

232 The boundary is discretized into twenty quadratic elements. For the interior points
 233 increasingly close to the boundary, the results of the radial and tangential stresses,
 234 σ_r and σ_θ , on the line $x_2 = 0$ are listed in Tab. 5 and Tab. 6, respectively. It can
 235 be observed that the values of the interior stresses obtained by using the CBEM be-
 236 come deviated when $x_1 < 5.2$. In contrast, the present method can obtain excellent

237 results with the largest relative error less than 0.06% for radial stresses and 0.2%
 238 for tangential stresses even when $x_1 = 5.0000000001$.

Table 5: Radial stresses σ_r at interior points on the line $x_2 = 0$

Radius r	Exact	CBEM	Present	Relative error
5.2	-0.462278E+01	-0.4590583E+01	-0.4621969E+01	0.1757317E-01
5.1	-0.480584E+01	-0.3778935E+01	-0.4805366E+01	0.9943386E-02
5.01	-0.498006E+01	0.3201157E+01	-0.4980010E+01	0.9963969E-03
5.001	-0.499800E+01	0.3696937E+01	-0.4997996E+01	0.9480385E-04
5.0001	-0.499980E+01	0.3743547E+01	-0.4999791E+01	0.1804154E-03
5.00001	-0.499998E+01	0.3748205E+01	-0.5000032E+01	0.1049353E-02
5.000001	-0.499999E+01	0.3748671E+01	-0.4999921E+01	0.1531263E-02
5.0000001	-0.500000E+01	0.3748718E+01	-0.4999513E+01	0.9744626E-02
5.00000001	-0.500000E+01	0.3748722E+01	-0.5000367E+01	0.7330816E-02
5.000000001	-0.500000E+01	0.3748723E+01	-0.5002389E+01	0.4778081E-01
5.0000000001	-0.500000E+01	0.3748723E+01	-0.5002995E+01	0.5990278E-01

Table 6: Tangential stresses σ_θ at interior points on the line $x_2 = 0$

Radius r	Exact	CBEM	Present	Relative error
5.2	0.4622781E+01	0.4600389E+01	0.4624871E+01	-0.4521102E-01
5.1	0.4805844E+01	0.4163711E+01	0.4809111E+01	-0.6798521E-01
5.01	0.4980060E+01	0.6704914E+01	0.4984544E+01	-0.9004280E-01
5.001	0.4998001E+01	0.8542143E+01	0.5002605E+01	-0.9213396E-01
5.0001	0.4999800E+01	0.8732868E+01	0.5004408E+01	-0.9217102E-01
5.00001	0.4999980E+01	0.8751950E+01	0.5004650E+01	-0.9339370E-01
5.000001	0.4999998E+01	0.8753859E+01	0.5004510E+01	-0.9023574E-01
5.0000001	0.5000000E+01	0.8754049E+01	0.5004211E+01	-0.8422029E-01
5.00000001	0.5000000E+01	0.8754068E+01	0.5005206E+01	-0.1041124E+00
5.000000001	0.5000000E+01	0.8754070E+01	0.5006909E+01	-0.1381724E+00
5.0000000001	0.5000000E+01	0.8754071E+01	0.5006582E+01	-0.1316304E+00

239 In addition, the convergence rates of the radial and tangential stresses, σ_r and σ_θ ,
 240 at the point $(5.0000001, 0)$ are shown in Fig. 12, from which we can observe that
 241 the convergence rates of the computed stresses σ_r and σ_θ are acceptable even when
 242 the distance between the computed point and the boundary reaches 10^{-7} .

243 6 Conclusions

244 In the present paper, a general strategy based on a nonlinear transformation is pro-
 245 posed in order to calculate the nearly singular integrals occurring on high-order
 246 geometrical elements. The strategy produces very high accuracy for determining
 247 the nearly singular integrals even when the distance between the field points and
 248 the integral elements are as small as $1.0E - 9$. Three numerical examples show that
 249 the present algorithm has been successfully employed in the numerical calculation
 250 of nearly singular integrals on curved elements. As a result, accurate stress results
 251 of the interior points close to the boundary are achieved. The present method is
 252 also general and can be applied to other problems in BEM (such as thin-walled
 253 structures), which will be discussed later.

254 **Acknowledgement:** The research is supported by the National Natural Science
 255 Foundation of China (no. 10571110) and the Natural Science Foundation of Shan-
 256 dong Province of China (no. 2003ZX12).

257 References

- 258 **Albuquerque, E.L.; Aliabadi, M.H.** (2008): A Boundary Element Formulation
 259 for Boundary Only Analysis of Thin Shallow Shells. *CMES: Computer Modeling*
 260 *in Engineering and Sciences*, vol. 29, no. 2, pp. 63-73.
- 261 **Atluri, S.N.** (2004a): *The meshless method (MLPG) for domain and BIE dis-*
 262 *cretizations*.
 263 Forsyth, GA, USA, Tech Science Press.
- 264 **Atluri, S.N.** (2005): *Methods of computer modeling in engineering and the sci-*
 265 *ences*. Tech Science Press.
- 266 **Atluri, S.N.; Han, Z.D.; Rajendran, A.M.** (2004b): A new implementation of
 267 the meshless finite volume method through the MLPG “mixed” approach. *CMES:*
 268 *Computer Modeling in Engineering and Sciences*, vol. 6, no. 6, pp. 491-514.
- 269 **Atluri, S.N.; Liu, H.T.; Han, Z.D.** (2006): Meshless local Petrov-Galerkin (MLPG)
 270 mixed collocation method for elasticity problems. *CMES: Computer Modeling in*
 271 *Engineering and Sciences*, vol. 14, no. 3, pp. 141-152.
- 272 **Brebbia, C.A.; Tells, J.C.F.; Wrobel, L.C.** (1984): *Boundary Element Tech-*
 273 *niques*. Berlin, Heidelberg, New York, Tokyo: Springer.
- 274 **Cerrolaza, M.; Alarcon, E.** (1989): A bi-cubic transformation of the Cauchy prin-
 275 cipal value integrals in boundary methods. *Int J Numer Methods Engng*, vol. 28,
 276 pp. 987-999.
- 277 **Chen, H.B.; Lu, P.; Huang, M.G.; Williams, F.W.** (1998): An effective method

- 278 for finding values on and near boundaries in the elastic BEM. *Comput Struct*, vol.
279 69(4), pp. 421-431.
- 280 **Chen, J.T.** (2000): Recent development of dual BEM in acoustic problems. *Com-*
281 *put Methods Appl Mech Eng*, vol. 188, pp. 833-845.
- 282 **Chen, J.T.; Chen, K.H.; Chen, C.T.** (2002): Adaptive boundary element method
283 of time-harmonic exterior acoustics in two dimensions. *Comput Methods Appl*
284 *Mech Eng*, vol. 191, pp. 3331–3345.
- 285 **Chen, X.L.; Liu, Y.J.** (2001): Thermal stress analysis of multi-layer thin films and
286 coatings by an advanced boundary element method. *CMES: Computer Modeling*
287 *in Engineering and Sciences*, vol. 2(3), pp. 337–49.
- 288 **Cruse, T.A.** (1974): An improved boundary integral equation method for three
289 dimensional elastic stress analysis. *Compt Struct*, vol. 4, pp. 741-754.
- 290 **Cruse, T.A.; Aithal, R.A.** (1993): A new integration algorithm for nearly singular
291 BIE kernels. *Int J Numer Methods Eng*, vol. 36, pp. 237-254.
- 292 **Davies, A.J.; Crann, D.; Kane, S.J.; Lai, C.H.** (2007): A Hybrid Laplace Trans-
293 form/Finite Difference Boundary Element Method for Diffusion Problems. *CMES:*
294 *Computer Modeling in Engineering and Sciences*, vol. 18, no. 2, pp. 79-85.
- 295 **Earlin, L.** (1992): Exact Gaussian quadrature methods for near-singular integrals
296 in the boundary element method. *Eng Anal Bound Elem*, vol. 9, pp. 233-245.
- 297 **Earlin, L.** (1993): A mapping method for numerical evaluation of two-dimensional
298 integrals with singularity. *Comput Mech*, vol. 12, pp. 19- 26.
- 299 **Fratantonio, M.; Rencis, J.J.** (2000): Exact boundary element integrations for
300 two-dimensional Laplace equation. *Eng Anal Bound Elem*, vol. 24, pp. 325–42.
- 301 **Friedrich, F.** (2002): A linear analytical boundary element method for 2D homo-
302 geneous potential problems. *Comput Geosci*, vol. 28, pp. 679–92.
- 303 **Gao, X.W.; Yang, K.; Wang, J.** (2008): An adaptive element subdivision tech-
304 nique for evaluation of various 2D singular boundary integrals. *Eng Anal Bound*
305 *Elem*, vol. 32, pp. 692–696.
- 306 **Gray, L.J.; Garzon, M.; Mantic, V.E.** (2006): Graciani, Galerkin boundary in-
307 tegral analysis for the axisymmetric Laplace equation. *Int J Numer Methods Eng*,
308 vol. 66, pp. 2014–2034.
- 309 **Granados, J.J.; Gallego, G.** (2001): Regularization of nearly hypersingular inte-
310 grals in the boundary element method. *Eng Anal Bound Elem*, vol. 25, pp. 165-
311 184.
- 312 **Guiggiani, M.; Krishnasamy, G.; Rudolphi, T.J.; Rizzo, F.J.** (1992): A general
313 algorithm for the numerical solution of hypersingular BEM. *J Appl Mech*, vol. 59,

- 314 pp. 604- 627.
- 315 **Guz, A.N.; Menshykov, O.V.; Zozulya, V.V.; Guz, I.A.** (2007): Contact Problem
316 for the Flat Elliptical Crack under Normally Incident ShearWave. *CMES: Com-*
317 *puter Modeling in Engineering and Sciences*, vol. 17, no. 3, pp. 205-214.
- 318 **Huang, Q.; Cruse, T.A.** (1993): Some notes on singular integral techniques in
319 boundary element analysis. *Int J Numer Methods Engng*, vol. 36, pp. 2643-2659.
- 320 **Johnston, P.R.** (1999): Application of sigmoidal transformations to weakly singu-
321 lar and near singular boundary element integrals. *Int J Numer Meth Eng*, vol. 45,
322 pp. 1333-1348.
- 323 **Johnston, P.R.** (2000): Semi-sigmoidal transformations for evaluating weakly sin-
324 gular boundary element integrals. *Int J Numer Meth Eng*, vol. 47, pp. 1709-1730.
- 325 **Jun, L.; Beer, G.; Meek** (1985): Efficient evaluation of integrals of order using
326 Gauss quadrature. *Engng Anal*, vol. 2, pp. 118-23.
- 327 **Karlis, G.F.; Tsinopoulos, S.V.; Polyzos, D.; Beskos, D.E.** (2008): 2D and 3D
328 Boundary Element nalysis of Mode-I Cracks in Gradient Elasticity. *CMES: Com-*
329 *puter Modeling in Engineering and Sciences*, vol. 26, no. 3, pp. 189-207.
- 330 **Lachat, J.C.; Watson, J.O.** (1976): Effective numerical treatment of boundary
331 integral equation: a formulation for elastostatics. *Int J Numer Meth Eng*, vol. 21,
332 pp. 211-228.
- 333 **Li, J.; Wu, J.M.; Yu, D.H.** (2009): Generalized Extrapolation for Computation of
334 Hypersingular Integrals in Boundary Element Methods. *CMES: Computer Model-*
335 *ing in Engineering and Sciences*, vol. 42, no. 2, pp. 151-175.
- 336 **Lifeng, M.A.; Alexander, M.; Korsunsky** (2004): A note on the Gauss-Jacobi
337 quadrature formulae for singular integral equations of the second kind. *Int J Fract*,
338 vol. 126, pp. 339-405.
- 339 **Liu, C.S.; Chang, C.W.; Chang, J.R.** (2008): A New Shooting Method for Solv-
340 ing Boundary Layer Equations in Fluid Mechanics. *CMES: Computer Modeling in*
341 *Engineering and Sciences*, vol. 32, no. 1, pp. 1-15.
- 342 **Liu, Y.J.** (1998): Analysis of shell-like structures by the boundary element method
343 based on 3-D elasticity: formulation and verification. *Int J Numer Meth Engng*,
344 vol. 41, pp. 541-558.
- 345 **Luo, J.F.; Liu, Y.J.; Berger, E.J.** (1998): Analysis of two- dimensional thin struc-
346 tures (from micro- to nano-scales) using the boundary element method. *Comput*
347 *Mech*, vol.22, pp. 404-412.
- 348 **Ma, H.; Kamiya, N.** (2002): Distance transformation for the numerical evalua-
349 tion of near singular boundary integrals with various kernels in boundary element
350 method. *Eng Anal Bound Elem*, vol.26, pp. 329- 339.

- 351 **Mukherjee, S.; Chati, M.K.; Shi, X.L.** (2000): Evaluation of nearly singular inte-
352 grals in boundary element contour and node methods for three-dimensional linear
353 elasticity. *Int J Sol Struct*, vol. 37, pp. 7633-7654.
- 354 **Niu, Z.R.; Cheng, C.Z.; Zhou, H.L.; Hu, Z.J.** (2007): Analytic formulations
355 for calculating nearly singular integrals in two-dimensional BEM. *Eng Anal Bound*
356 *Elem*, vol. 31, pp. 949-964.
- 357 **Sanz, J.A.; Solis, M.; Dominguez, J.** (2007): Hypersingular BEM for Piezoelec-
358 tric Solids: Formulation and Applications for FractureMechanics. *CMES: Com-*
359 *puter Modeling in Engineering and Sciences*, vol. 17, no. 3, pp. 215-229.
- 360 **Sladek, V.; Sladek, J.; Tanaka, M.** (1993): Regularization of hypersingular and
361 nearly singular integrals in the potential theory and elasticity. *Int J Numer Methods*
362 *Eng*, vol. 36, pp. 16-28.
- 363 **Sladek, V.; Sladek, J.; Tanaka, M.** (2000): Optimal transformations of the inte-
364 gration variables in computation of singular integrals in BEM. *Int J Numer Methods*
365 *Eng*, vol. 47, pp. 1263-1283.
- 366 **Sun, H.C.; Zhang, L.Z.; Xu, Q.; Zhang, Y.M.** (1999): *Nonsingular Boundary*
367 *Element Method*. Dalian: Dalian University of Technology Press (in Chinese).
- 368 **Tanaka, M.; Matsumoto, T.; Nakamura, M.** (1991): *Boundary element method*.
369 Baifukan Press, Tokyo (in Japanese).
- 370 **Tanaka, M.; Sladek, V.; Sladek, J.** (1994): Regularization techniques applied to
371 BEM. *Appl Mech Rev*, vol. 47, pp. 457-499.
- 372 **Telles, J.C.F.** (1987): A self-adaptive coordinate transformation for efficient nu-
373 merical evaluation of general boundary element integral. *Int J Numer Meth Eng*,
374 vol. 24, pp. 959-973.
- 375 **Wang, Y.C.; Li, H.Q.; Cheng, H.B.; Wu, Y.** (1994) Calculating the stresses and
376 displacements at arbitrary points with the particular solution field method. *Acta*
377 *Mech Sin*, vol. 26(2), pp. 222-231.
- 378 **Yoon, S.S.; Heister, S.D.** (2000): Analytic solution for fluxes at interior points for
379 2D Laplace equation. *Eng Anal Bound Elem*, vol. 24, pp. 155-60.
- 380 **Young, D.L.; Chen, K.H.; Chen, J.T.; Kao, J.H.** (2007): A Modified Method of
381 Fundamental Solutions with Source on the Boundary for Solving Laplace Equa-
382 tions with Circular and Arbitrary Domains. *CMES: Computer Modeling in Engi-*
383 *neering and Sciences*, vol. 19, no. 3, pp. 197-221.
- 384 **Zhang, Y.M.; Wen, W.D.** (2004): A kind of new nonsingular boundary integral
385 equations for elastic plane problems. *Acta Mech*, vol.36(3), pp. 311-321 (in Chi-
386 nese).
- 387 **Zhang, Y.M.; Sun, C.L.** (2008): A general algorithm for the numerical evalua-

- 388 tion of nearly singular boundary integrals in the equivalent non-singular BIES with
389 indirect unknowns. *Journal of the Chinese Institute of Engineers*, vol. 31, pp.
390 437-447.
- 391 **Zhang, Y.M.; Sun, H.C.** (2001): Analytical treatment of boundary integrals in
392 direct boundary element analysis of plane potential and elasticity problems. *Appl*
393 *Math Mech*, vol. 6, pp. 664-673.
- 394 **Zhang, Y.M.; Sun, H.C.** (2000): Theoretic Analysis on Virtual Boundary Element.
395 *Chinese J Comp Mech*, vol.17, pp. 56-62 (in Chinese).
- 396 **Zhang, X.S.; Zhang, X.X.** (2004): Exact integrations of two-dimensional high-
397 order discontinuous boundary element of elastostatics problems. *Eng Anal Bound*
398 *Elem*, vol. 28, pp. 725-732.
- 399 **Zhou, H. L.; Niu, Z. R.; Cheng, C. Z.** (2008): Analytical integral algorithm ap-
400 plied to boundary layer effect and thin body effect in BEM for anisotropic potential
401 problems. *Comp and Struct*, vol.86, pp. 1656– 1671.

Proof